Comparative Study of W-Band DDR IMPATTs Based on $Si/Si_{1-x}Ge_x$ and Si at Different Bias Current Density

S.J.Mukhopadhyay, S.Rani, M.Mitra

Abstract—In this paper a comparative study has been made on DDR IMPATT diodes based on heterojunction $Si/Si_{1-x}Ge_x$ and its conventional homojunction Si for different bias current density operating at W-band window frequency. In this case the value of x, the Ge mole fraction, is taken to be 0.1. A double iterative computer method based on drift-diffusion model has been used to study the DC and small signal admittance properties of the device. The simulation studies show that heterojunction $Si/Si_{1-x}Ge_x$ based DDR IMPATTs produce much better performance than its homojunction Si counterpart with regards to DC to RF conversion efficiency.The maximum DC to RF conversion efficiency for $Si/Si_{1-x}Ge_x$ is found to be 16.11% at bias current density of $2.2x10^8 A/m^2$ whereas for Si based IMPATTs, maximum conversion efficiency of 10.67% is obtained at bias current density of $3.4x10^8 A/m^2$. The design results presented in this paper will be highly useful to realize experimentally Si/Si1-xGex IMPATTS for W-Band window frequency.

Index Terms— Bias current density, Conversion efficiency, Double drift IMPATT diode, Si, Si/Si1-xGex, W band IMPATT diode.

1 Introduction

THE W-band of the microwave part of the electromagnetic spectrum ranges from 75-110 GHz, wavelength about 2.7-4mm.The W-band is used for satellite communications, millimeter-wave radar research, military radar targeting and tracking applications and some non-military applications. A number of passive millimeter wave cameras for concealed weapons detection operate at 94GHz.The atmospheric radio window at 94GHz is used for imaging millimeter-wave radar applications in astronomy, defense and security applications.

Among all the solid state sources, IMPATT diode have already emerged as the most efficient source for its ability to deliver high RF power even at 300GHz or more. It is wellknown that RF power depends on various factors like critical field for avalanche breakdown, saturation drift velocity for charge carriers etc which varies for different semiconductor materials and play vital role in limiting the output power of an IMPATT diode at a particular operating frequency. The rapid development of Silicon technology in the decade of seventies has made possible the practical realization of Silicon based single drift (SDR) and double drift (DDR) IMPATT devices capable of providing RF output power of the order of several watts at microwave and millimeter wave frequency bands [1-4].

- *S.J.Mukhopadhyay is currently pursuing PhD program in electronics and Telecommunication engineering in Indian Institute of Engineering Science and Technology, Shibpur, Howrah, India, PH-09800206211. E-mail: jana_sangeeta@yahoo.co.in*
- *S.Rani is currently pursuing M.Tech in electronics and Telecommunication engineering in Indian Institute of Engineering Science and Technology, Shibpur, Howrah, India.*
- *M.Mitra is currently working as Professor and H.O.D in electronics and Telecommunication engineering in Indian Institute of Engineering Science and Technology, Shibpur, Howrah, India.*

However, the driving force behind today's growth in high speed optical networking, inexpensive, light weight personal communication devices is not silicon but silicon-germanium (SiGe). This technology increases operating speed, reduces electronic noise, lowers power consumption, supports higher levels of integration and thus enables the design of more functional components on a chip. The number of SiGe applications is expected to explore over the next few years. SiGe involves a revolutionary process technology in which the electrical properties of silicon are augmented with germanium to make the chips operate more efficiently. As such, SiGe offers a bridge between low cost, low power, low frequency silicon chips and high cost, high power, high frequency chips made from class III-V semiconductor materials such as GaAs and InP. Unlike the manufacture of other high-speed semiconductors made of two or more materials, SiGe processing is relatively simple because silicon and germanium have similar chemical and physical properties. As silicon does not operate at frequencies above a few gigahertz, it has hampered the development of higher speed wireless telecommunication devices. In contrast to silicon based chips, SiGe semiconductors have much higher speed. Si1-xGex layers on Si has been developed for the fabrication of heterojunction bipolar transistors (HBTs), Bipolar complementary MOS (BiCMOS), Modulation Doped Field Effect Transistors (MODFETs) and Infrared Photoconductors that operate into the millimeter wave frequency spectrum which make Si1-xGex a viable material for microwave and millimeter wave source and related circuit applications. Thus undoubtedly, Si1-xGex with Si has come up as technologically important material combination for both electronic and opto-electronic devices [5-9].

Here in this paper, a comparison of $Si/Si_{1-x}Ge_x$ heterojunction DDR IMPATT with similar Si homojunction counterpart has

been investigated.

2 MATERIAL PARAMETERS AND DESIGN METHOD

2.1 Material Parameter

The $Si/Si_{1-x}Ge_x$ heterojunction DDR IMPATT diode under consideration has n+ = Si, n = Si, p = $Si/Si_{1-x}Ge_x$, p+ = $Si/Si_{1-x}Ge_x$ the Ge mole fraction x=0.1.The variation of bandgap with Ge mole fraction x for unstrained $Si/Si_{1-x}Ge_x$ grown is given by Eg(x) = 1.12 – 0.46x. The dielectric constant for Si and Ge is 11.9 and 16.0 respectively and that of unstrained $Si/Si_{1-x}Ge_x$ layer grown on a <100> Si substrate is given by ε(x) =11.9 + 4.1x. The electron and hole mobility of $Si/Si_{1-x}Ge_x$ is calculated from the method described elsewhere [10, 11].

The electric field variation of carrier ionization rates in Si and $Si/Si_{1-x}Ge_x$ are given by

$$\alpha n,p(\zeta)=An,pexp[(-Bn,p/\zeta)m]$$

Where the value of constant m=1 for both Si and $Si/Si_{1-x}Ge_x$.The values of An,p and Bn,p for Si have been taken from the experimental results reported by Grant 1973[12] and the values of An,p and Bn,p for $Si/Si_{1-x}Ge_x$ at 300K are obtained from the data of Lee,1996 [13].The electron and hole drift velocity versus field characteristics of Si and $Si/Si_{1-x}Ge_x$ have an experimental field dependence given by

$$vn,p(\zeta)=vsn,sp[1-exp(-\mu n,p\zeta/vsn,sp)]$$

The values of vsn and vsp for Si and $Si/Si_{1-x}Ge_x$ are taken from the data of Canali[14] and Thomber,1980[15].

All other material parameters such as bandgap(Eg), intrinsic carrier concentration(ni), effective density of states of conduction and valance bands(Nc,Nv), diffusion coefficients(Dn,Dp), mobilities(μn,μp) and diffusion lengths(Ln,Lp) of charge carriers and permittivity(εs) of the semiconductor materials under consideration are taken from published reports Electronic Archive[16].

2.2 Design-Method

The frequency of operation of an IMPATT device essentially depends on the transit time (τ_T) of charge carriers to cross the depletion layer of the device. IMPATT devices having double-drift n+-n-p-p+ structure are first designed for a particular frequency (fd) from the transit time formula of Sze and Ryder [17] given by Wn,p = 0.37 vsn,sp / fd; where Wn,p is the width of n- and p-drift region, and vsn,sp is the saturation drift velocity of electrons, holes respectively. Here n+- and p+-layers are highly doped layers whose doping concentrations are taken to be Nn+ = Np+=1026 m-3. The background doping concentrations of n- and p-depletion regions (ND, NA) are initially chosen according to the design frequency, fd.The design frequency is taken to be 94 GHz at W-band in the present simulation study.Using the above design doping and structural parameters the electric field profile is obtained from a double-iterative field maximum simulation technique reported earlier [18]. The doping parameters and corresponding structural parameters are adjusted till the simulated electric field profile just punches through the depletion layers (Wn, Wp) corresponding to the design frequency, fd at a particular biasing current density, J0. A small-signal simulation method described in [19] is used to find out the high frequency admittance and negative resistance properties of the device. This method is based on Gummel-Blue approach [20]. The optimum frequency (fp) corresponding to the peak negative conductance (Gp) is determined from the simulated admittance characteristics of the device. If the magnitude of fp differs very much from fd, the value of J0 is varied and the computer simulation program is run till the value of fp is nearly equal to the value of fd. The bias current density, J_0 is thus fixed for a particular design frequency. Realistic doping profile for flat profile DDR IMPATT diode has been used in the present analysis. The doping profile at the interface of epitaxy and substrate (i.e. n+n-interface) is approximated to be error function. The doping profile near the p+p-interface is made realistic by suitable exponential function.

Here for a fixed current density ($3.4x10^8$Am-2) design parameters are shown for Si and $Si/Si_{1-x}Ge_x$ below in the table1.

TABLE 1

	Si	$Si/Si_{1-x}Ge_x$
Width of n-epilayer(μm)	0.390	0.380
Width of p-epilayer(μm)	0.390	0.360
Background doping concentration(1023 m-3)	1.25	0.75
Current density(108 Am-2)	3.4	3.4
Substrate doping concentration(1026 m-3)	1.0	1.0

3 PROPOSED ANALYSIS MODEL

One-dimensional model of reverse biased n+-n-p-p+ lateral homojunction Si and heterojunction $Si/Si_{1-x}Ge_x$ based DDR IMPATT structure, shown in Fig. 1 and Fig.2 are used to simulate the DC and high frequency properties of the device. The physical phenomena take place in the semiconductor bulk along the symmetry axis of the DDR IMPATT devices. Thus the one-dimensional model of IMPATT devices considered in this work is justified.

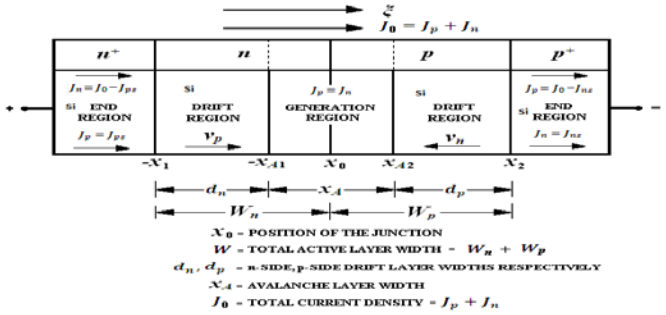

Fig. 1. One-dimensional model of Si based DDR IMPAT device

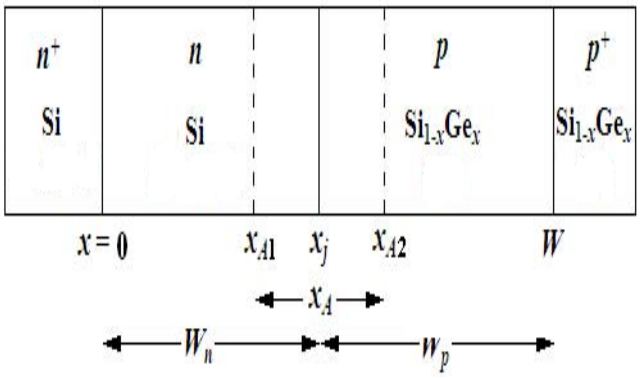

Fig. 2. One-dimensional model of $Si/Si_{1-x}Ge_x$ based DDR IMPATT device

DC and High Frequency Simulation

The DC electric field and normalized current density profiles in the depletion layer of the device are obtained from simultaneous numerical solution of fundamental device equations such as Poisson's equation, combined carrier continuity equation, current density equations and mobile space charge equation subject to appropriate boundary conditions.The simulation method starts with DC analysis described in details elsewhere [19]. In this method, the computation starts from the field maximum near the metallurgical junction. The distribution of DC electric field and carrier currents in the depletion layer is obtained by the double-iterative computer method, which involves iteration over the magnitude of field maximum(Em) and its location in the depletion layer. A computer algorithm has been developed for simultaneous numerical solution of Poisson's equation, carrier continuity equations and the space charge equation taking into account the effect of mobile space charge and carrier diffusion in order to obtain the electric field profiles and carrier current profiles. The boundary conditions for the electric field at the depletion layer edges are given by

$$\xi(-x_1)=0 \text{ and } \xi(x_2)=0 \quad (1)$$

Where $-x_1$ and x_2 define the p+ and n+ edges of the depletion layer. Similarly the boundary conditions for normalized difference of hole and electron current density, P(x) = (Jp(x) – Jn(x)) / J0 (where J0 = Jp + Jn) at the depletion layer edges i.e., at x = -x1 and x = x2 are given by:

$$P(-x_1)=(2/Mp-1) \text{ and } P(x_2)=(1-2/Mn) \quad (2)$$

where Mn and Mp are the electron and hole multiplication factors. The field dependence of electron and hole ionization rates and saturated drift velocities of electron (vsn) and holes (vs, p) at 300K are made use of in the computation for the profiles of electric field and carrier currents [16].

The conversion efficiency is calculated from the approximate formula [21]

$$\eta(\%)=(1*Vd)/(\pi*VB) \quad (3)$$

The magnitude of peak field at the junction (ξp), the widths of avalanche and drift zones (xA and xD; where xD = dn + dp) and the voltage drops across these zones (VA, VD) are obtained from the DC simulation program. These values are fed back as input parameters in the small-signal simulation to obtain the high frequency admittance properties of the device. The depletion layer edges of the device are obtained from the output of DC simulation program. The edges of the depletion layer are then taken as the starting and end points of small-signal simulation program. Two second order differential equations are framed from Gummel-Blue model [20] by resolving the device impedance Z(x,ω) into its real part R(x,ω) and imaginary part X(x,ω); where Z(x,ω) = R(x,ω) + jX(x,ω). Two simultaneous second order differential equations in R and X are numerically solved by using Runge-Kutta method [20]. Double-iteration over the initial choice of the values of R and X at one edge is carried out till the boundary conditions for R and X are satisfied at the other edge [20]. The negative specific resistance (R(x)) and specific reactance (X(x)) profiles in the depletion layer of the device are obtained from the above solution. The device negative resistance (ZR) and reactance (ZX) are obtained from the numerical integration of the respective R(x)- and X(x)-profiles over the depletion layer width (W). The negative conductance (G) and susceptance (B) of the device at a particular frequency are computed from the following expressions:

$$-G=-ZR/[(ZR)2+(ZX)2] \text{ and } B=ZX/[(ZR)2+(ZX)2] \quad (4)$$

It may be noted that both G and B are normalized with respect to the junction area (Aj) of the device. The admittance characteristics i.e., G(ω) versus B(ω) plots of the device are obtained from the above analysis for different bias current

densities.

At a resonant frequency of oscillation, the maximum power output PRF from the device can be obtained from the following expression,

$$PRF=V_{RF}^2(Gp)A/2 \quad (5)$$

where,VRF is the amplitude of the RF swing and is taken as VB/2,assuming 50% modulation of the breakdown voltage VB. Gp is the diode negative conductance at the operating frequency and A is the area of the diod,taken as 10^-10 m^2.

4 RESULTS AND DISCUSSIONS

The various DC and high frequency properties of Si and Si/Si1-xGex based DDR IMPATT diodes are obtained from simulation studies at W-band window frequency 94 GHz given in table II and table III.It is observed from table2 and table3 that peak electric field (Em) at the junction decreases with increase in bias current density for both Si and Si/Si1-xGexbased IMPATTs.The E(x) profiles at high bias current levels are found to be punch through type for Si and Si/Si1-xGex based DDR IMPATTs as shown in fig.3 and fig.4.The bias current density for maximum efficiency of 10.67% and 16.11% is found to be 3.4*108Am-2 and 2.2*108Am-2 in Si and Si/Si1-xGex based DDR IMPATTs respectively.It is also observed from fig.7 below that DC to RF conversion efficiency increases with bias current density for Si based IMPATT diodes,whereas for heterojunction Si/Si1-xGex based IMPATTs,conversion efficiency decreases with bias current density.Admittance characteristics or high frequency conductance-susceptance plots of Si and Si/Si1-xGex based DDRs are shown in fig5 ang fig6.It is interesting to observe that from table 2 and table 3, the magnitude of ZR is higher for Si based IMPATTs than Si/Si1-xGex IMPATTs.Higher magnitude of Negative resistance implies higher output power,naturally higher value of RF power output(PRF) is obtained for conventional Si based DDR IMPATTs than heterostructure Si/Si1-xGex.

TABLE 2

DC AND SMALL SIGNAL PROPERTIES OF SI IMPATT

	J=2.2*10⁸ A/m²	J=2.6*10⁸ A/m²	J=3.0*10⁸ A/m²	J=3.4*10⁸ A/m²
Em(*108 V/m)	0.6087	0.6062	0.6037	0.6012
Breakdown voltage(V)	23.04	23.38	23.92	24.31
Efficiency (%)	10.20	10.27	10.49	10.67
Gp(*107 Sm-2)	-3.462	-3.883	-3.720	-4.334
ZR(*10-9 Ωm-2)	-5.331	-5.655	-6.859	-7.130
Quality factor(-Q)	2.101	1.884	1.708	1.495
P_{RF}(W)	0.2297	0.2653	0.2660	0.3202

TABLE 3

DC AND SMALL SIGNAL PROPERTIES OF SI/SI1-XGEX IMPATT

	J=2.2*10⁸ A/m²	J=2.6*10⁸ A/m²	J=3.0*10⁸ A/m²	J=3.4*10⁸ A/m²
Em(*108 V/m)	0.3556	0.3543	0.3525	0.3506
Breakdown voltage(V)	14.60	15.06	15.49	15.88
Efficiency (%)	16.11	15.52	15.30	14.63
Gp(*107 Sm-2)	-0.1919	-0.1997	-0.2048	-0.2036
ZR(*10-9 Ωm-2)	-0.1709	-0.1731	-0.1672	-0.1529
Quality factor(-Q)	55.18	53.75	54.01	56.63
PRF(W)	0.0492	0.0545	0.05912	0.06184

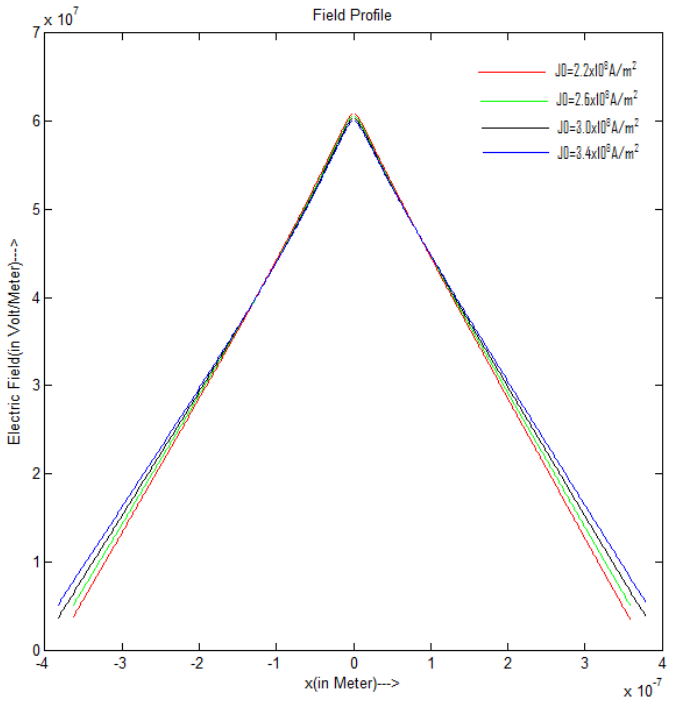

Fig. 3. Electric Field Profile for Si DDR IMPATT for different bias current density

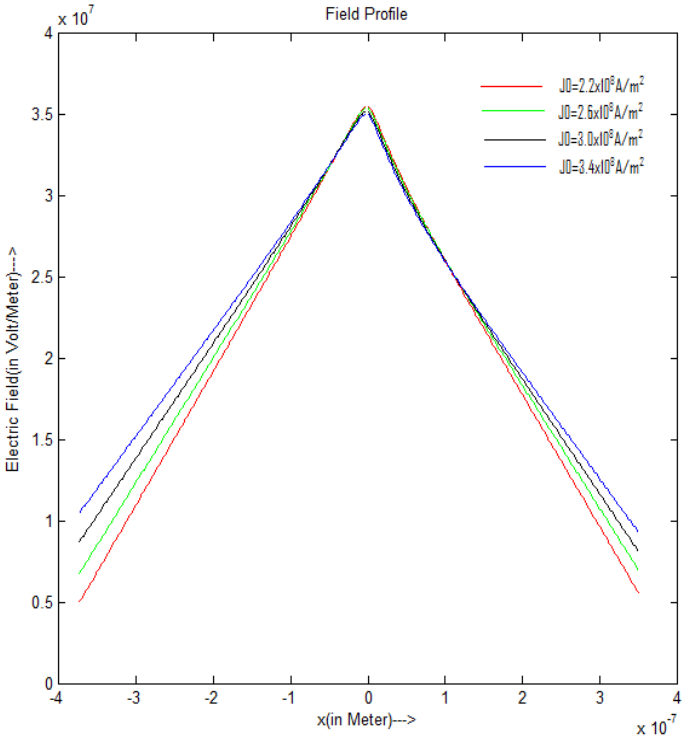

Fig. 4. Electric Field Profile for Si/Si1-xGex DDR IMPATT for different bias current density.

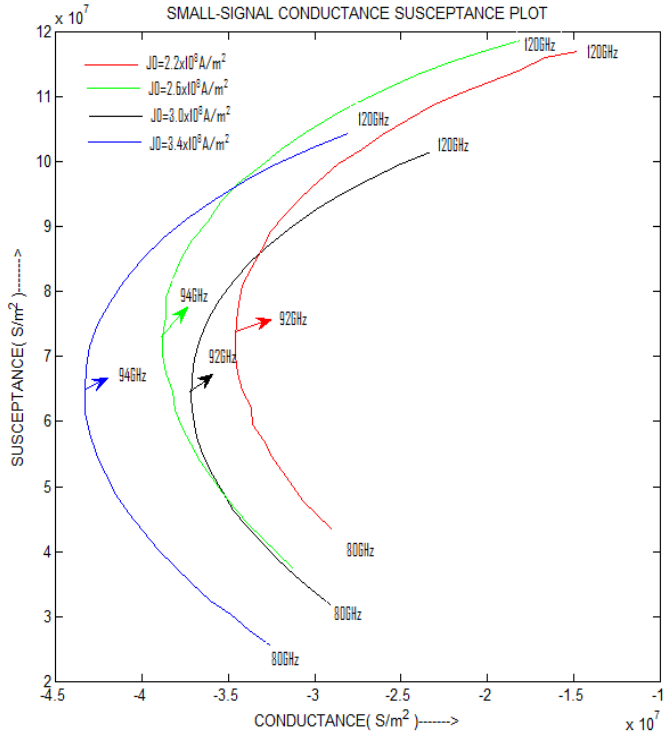

Fig. 5. Conductance-Susceptance plot for Si DDR IMPATT for different bias current density.

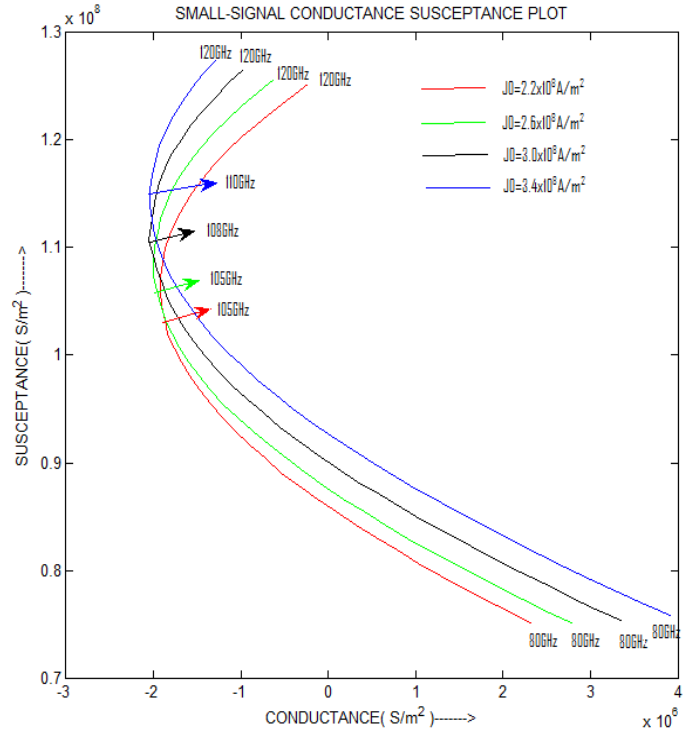

Fig. 6. Conductance-Susceptance plot for Si/Si1-xGex DDR IMPATT for different bias current density.

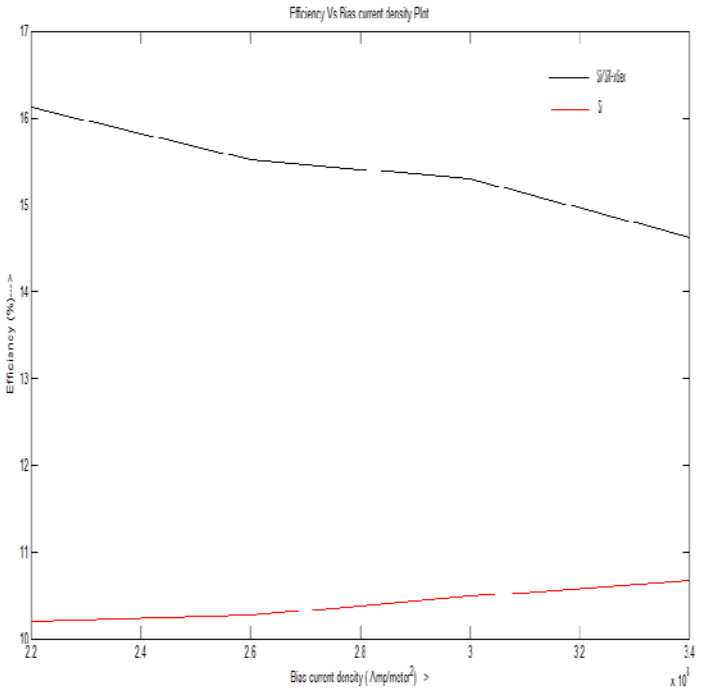

Fig. 7. EfficiencyVs.Bias current density plot for Si/Si1-xGex and Si DDR IMPATT.

5 CONCLUSION

The simulation results show that Si/Si1-xGex heterostructure DDR IMPATT diode exhibit higher efficiency than that of Si homostructure DDR IMPATT. The breakdown voltage for Si/Si1-xGex heterostructure DDR IMPATT is smaller in comparison to Si counterpart but owing to greater efficiency. Negative resistance at W-band is also generated in the unstrained Si/Si1-xGe IMPATT diode. Hence the results obtained are encouraging and clearly indicate that Si/Si1-xGex based IMPATT has also a great potential as mm-wave source.

ACKNOWLEDGMENT

The authors gratefully acknowledge the support rendered by Microwave research laboratory of IIEST (Indian Institute of Engineering Science and Technology), Shibpur, Howrah, W.B.

REFERENCES

[1] T.A.Midford and R.L.Bernick, "Millimeter-wave CW IMPATT Diodes and oscillators", IEEE Trans.Microwave Theory Tech., 27, 483, 1979.

[2] Y.Chang, J.M.Hellum, J.A.Paul and K.P.Weller, "Millimeter-wave IMPATT Sources for communication Application", IEEE MTT-S International Microwave Symposium Digest, 216-219, 1977.

[3] W.W.Gray, L.Kikushima, N.P.Morentc and R.J.Wagner, "Applying IMPATT Power sources to Modern Microwave Systems.", IEEE Journal of Solid-state Circuits, 4,409-413, 1969.

[4] Ray,U.C;Gupta,A.K.;Measurement of electrical series resistance of W band Si IMPATT diode.in 2nd Acia Pacific Microwave conference Proceedings, China, (1988), 434-437.

[5] Gruhle, "SiGe heterojunction bipolar transistors", in Silicon based Millimeterwave Devices (Series in Electronics & Photonics 32), J. F. Luy and P. Russer, Eds. Berlin, Germany, Springer-Verlag, 1994.

[6] Schuppen, H. Dietrich, U. Seiler, H. V. D. Ropp and U. Erben, "A SiGe RF technology for mobile communication systems", Microwave Engineering, Europe, pp. 39-46, June 1998.

[7] T. Masuda, K. Z. Ohhata, E. Ohne, K. Oda, M. Tanabe, H. Shimamota, T. Onai and K. Washio, "40 Gb/s analog IC chipset for optical receiver using SiGe HBT's", IEEE International Solid State Circuits Conference, pp. 314-315, 1998.

[8] W. Durr, U. Erben, A. Schuppen, H. Dietrich and H. Schumacher, "Low power, low noise active mixers for 5.7 and 11.2 GHz usingcommercialy available SiGe HNT MMIC technology", Electronics Letters, vol.34, no.12, pp. 1994-1996, 1998.

[9] M. K. M. Willander, "Optimised frequency characteristics of Si/SiGe heterojunction and conventional bipolar transistors", Solid State Electron., vol. 33, no. 2, pp. 199-204, 1990.

[10] Tajinder Manku and Arokia Nathan, "Electron drift mobility model based on unstrained and coherently strained Si1-xGex grown on <100> silicon substrate", IEEE ED, vol. 39, no. 9, 1992.

[11] Tajinder Manku, Joel M. McGregor and Arokia Nathan, "Drift hole mobility in strained and unstrained doped Si1-xGex alloys", IEEE ED, vol. 40, no. 11, 1992.

[12] Grant WN, "Electron and hole ionization rates in epitaxial silicon-solid state Electron", 16:1189-1203, 1973.

[13] J. Lee, A. L. Gutierrez-Aitken, S. H. Li, P. K. Bhattacharya, "Responsivity and impact ionisation Coefficients of Si1-xGex photodiodes", IEEE ED, vol. 43, no. 6, pp. 977-981, 1996.

[14] Canali C, Ottaviani G.Quaranta AA, "Drift velocity of electrons and holesand associated anisotropic effects in Silicon.", J Phys Chem Solids 32:1707,1971.

[15] K. K. Thomber, "Relation of drift velocity of low-field mobility andhigh field saturation velocity", J. Appl. Phys., vol. 51, pp. 2127-2136, 1980.

[16] Electronic Archive (2012) New semiconductor Materials, Characteristics and Properties.http;//www.ioffe.ru/SVA/NSM/semicond.

[17] SZE, S. M., RYDER, R. M. Microwave Avalanche Diodes. Proc. of IEEE, Special Issue on Microwave Semiconductor Devices, 1971, vol. 59, no. 8, p. 1140-1154

[18] ROY, S. K., SRIDHARAN, M., GHOSH, R., PAL, B. B. "Computer methods for the dc field and carrier current profiles in impatt devices starting from the field extremum in the depletion layer", Proc. of NASECODE-I Conf. on Numerical Analysis of Semiconductor Devices (Dublin: Boole Press), 1979, p. 266-274.

[19] S.K.Roy, J.P.Banerjee and S.P.Pati, "A Computer analysis of the distribution of high frequency negative resistance in the depletion layer of IMPATT Diodes", Proc.4th conf.on Num.Anal. of Semiconductor Devices(NASECODE IV)(Dublin)(Dublin:Boole),pp.494-500,1985.

[20] Gummel HK, Blue JL, "A Small –signal theory of avalanche noise in IMPATT diodes", IEEE Trans Electron Dev 14:5699-580.

[21] H. Eisele and G. I. Haddad, "Microwave Semiconductor Device Physics" (Ed. S. M. Sze), p. 343, Wiley, New York, 1997.